

The Small Scale Anisotropies, the Spectrum and the Sources of Ultra High Energy Cosmic Rays

Pasquale Blasi^{a,b,1} Daniel De Marco^{c,d,2}

^a*INAF/Osservatorio Astrofisico di Arcetri,
Largo E. Fermi, 5 - 50125 Firenze, ITALY*

^b*INFN/Sezione di Firenze, ITALY*

^c*Università degli Studi di Genova,
Via Dodecaneso, 33 - 16146 Genova, ITALY*

^d*INFN/Sezione di Genova, ITALY*

Abstract

We calculate the number density and luminosity of the sources of ultra high energy cosmic rays (UHECRs), using the information about the small scale anisotropies and the observed spectra. We find that the number of doublets and triplets observed by AGASA can be best reproduced for a source density of $\sim 10^{-5} \text{ Mpc}^{-3}$, with large uncertainties. The spectrum of UHECRs implies an energy input of $\sim 6 \times 10^{44} \text{ erg yr}^{-1} \text{ Mpc}^{-3}$ above 10^{19} eV and an injection spectrum $\propto E^{-2.6}$. A flatter injection spectrum, $E^{-2.4}$, can be adopted if the sources have luminosity evolution $\propto (1+z)^4$. The combination of these two pieces of information suggests that the single sources should on average have a cosmic ray luminosity above 10^{19} eV of $L_{\text{source}} \approx 2 \times 10^{42} \text{ erg s}^{-1}$, weakly dependent upon the injection spectrum. Unfortunately, with the limited statistics of events available at present, there are approximately one-two orders of magnitude uncertainty in the source density provided above. We make predictions on the expected performances of the Auger and EUSO experiments, with particular attention for the expected improvements in our understanding of the nature of the sources of UHECRs. We find that a critical experimental exposure Σ_c exists, such that experiments with exposure larger than Σ_c can detect at least one event from each source at energies above 10^{20} eV . This represents a unique opportunity to directly count and identify the sources of UHECRs.

¹ E-mail: blasi@arcetri.astro.it

² E-mail: ddm@ge.infn.it

1 Introduction

Despite the efforts in building several large experiments for the detection of particles with the highest energies in the cosmic ray spectrum, the nature of the sources of these particles and the acceleration processes at work are still unknown. No trivial counterpart has been identified by any of the current experiments: there is no significant association with any large scale local structure nor with single sources. However, caution should be adopted in looking for the sources and in claiming their absence: particles with energy around 4×10^{19} eV have a loss length of ~ 1000 Mpc, therefore many sources lie in the $\sim 2 - 3$ degrees of angular resolution of current experiments. It follows that the identification of one of them as responsible for the production of a single particle can turn out to be very difficult. In fact, for particles with this energy, one could say that there are too many possible sources that may potentially contribute, rather than the opposite. On the other hand, the need for statistically significant findings forces current experiments to work in this energy region. The events with energy above a few 10^{20} eV, where the loss length for photopion production is only $\sim 20 - 50$ Mpc are only a handful, but at least in principle it should be much simpler to find their sources. For instance, if we assumed that sources located within ordinary galaxies could accelerate particles to energy in excess of 10^{20} eV, one could easily estimate that in an angle of 2 degrees, at most ~ 1 galaxy should be within the near 20 Mpc from us. On the other hand, for particles with a pathlength 1000 Mpc, in the same angular bin there would be $\sim 4 \times 10^4$ galaxies.

It has been recently proposed that a statistically significant correlation may exist between the arrival directions of UHECRs with energy above 2×10^{19} eV and the spatial location of BL Lac objects, with redshifts larger than 0.1 [1,2]. Since at these energies the loss length is comparable with the size of the universe, no New Physics needs to be invoked to explain the correlation. On the other hand, since no BL Lac is known to be located close to the Earth, the spectrum of UHECRs expected from these sources would have a very pronounced GZK cutoff.

At the highest energies even the spectrum of UHECRs is measured rather poorly. The low expected number of events above 10^{20} eV does not allow a clear identification of the so-called GZK feature, caused by the sharp drop in the loss length of UHECRs at the onset of photopion production as the dominant channel of energy losses. In [3] it was shown that the two largest experiments, namely AGASA and HiRes [4,5], cannot measure the presence or lack of the GZK feature at a statistical level better than $\sim 2\sigma$. In the present paper, all the numbers quoted as expected numbers of events refer to the propagation of cosmic ray protons from astrophysical sources, therefore a GZK feature is present in all the spectra. If future experiments will show the

absence of the GZK feature in the spectrum of UHECRs, then many more events will be detected than predicted in this paper.

The potential for discovery of the sources has recently improved after the identification of a few doublets and triplets of events clustered on angular scales comparable with the experimental angular resolution of AGASA. A recent analysis of the combined results of most UHECR experiments [6] revealed 8 doublets and two triplets on a total of 92 events above 4×10^{19} eV (47 of which are from AGASA). The recent HiRes data do not show evidence for significant small angle clustering, but this might well be the consequence of the smaller statistics of events and of the energy dependent acceptance of this experiment: one should remember that in order to reconstruct the spectrum of cosmic rays, namely to account for the unobserved events, a substantial correction for this energy dependence need to be carried out in HiRes (the acceptance is instead a flat function of energy for AGASA at energies above 10^{19} eV). This correction however does not give any information on the spatial distribution of the *missed* events.

If the appearance of these multiplets in the data will be confirmed by future experiments as not just the result of a statistical fluctuation or focusing in the galactic magnetic field [7], then the only way to explain their appearance is by assuming that the sources of UHECRs are in fact point sources. This would represent the first true indication in favor of astrophysical sources of UHECRs, since the clustering of events in most top-down scenarios for UHECRs seems unlikely. A clear identification of the GZK feature in the spectrum of UHECRs would make the evidence in favor of astrophysical sources even stronger.

Previous attempts to estimate the number of sources of UHECRs in our cosmic neighborhood from the small scale anisotropies found by AGASA have been carried out, adopting both semi-analytical and numerical approaches. An analytical tool to evaluate the chance coincidence probability for arbitrary statistics of events was proposed in [8]. A rigorous analysis of the clusters of events and of their energy dependence was given in [9]. In [10] the authors use an analytical method to estimate the density of the sources of UHECRs restricting their attention to the 14 events with energy above 10^{20} eV with one doublet. They obtain a rather uncertain estimate centered around 6×10^{-3} Mpc $^{-3}$. In [11] the energy losses are introduced through a function, derived numerically, that provides the probability of arrival of a particle from a source at a given distance. Again, only events above 10^{20} eV are considered, therefore the analysis is based upon one doublet of events out of 14 events. This causes extremely large uncertainties in the estimate of the source density, found to be $180_{-165}^{+2730} \times 10^{-3}$ Mpc $^{-3}$. No account of the statistical errors in the energy determination nor of the declination dependence of the acceptance of the experimental apparatus is included in all these investigations. In the present paper we address the issue of calculating the number density and

luminosity of the sources of UHECRs with a full numerical simulation of the propagation, and we take into account the statistical errors in the energy determination and the declination dependence of the experiments involved. We carry out our analysis for cosmic rays detected by AGASA, with energy above 4×10^{19} eV, where the statistics of events is more generous. We also apply the same analysis to mock catalogs of events from Auger [12] and EUSO [13], with the statistics of events expected for each. Different tools are proposed to determine with some accuracy the density of the sources of UHECRs. We will present our results with magnetic fields in a forthcoming paper, extending recent interesting findings reported in [14,15] to the case of time dependent sources of UHECRs. The propagation of UHECRs in magnetic fields was also investigated in [16], where the important concept of magnetic horizon was introduced, and in [17,18] where special attention was devoted to the local neighborhood, although the contribution of distant sources was not considered.

The paper is organized as follows: in §2 we provide a description of the simulations used to propagate particles from point sources distributed throughout the universe. In §3 we use observational data and simulations to constrain the number of sources in the near universe and their luminosity. We also discuss at length several tools that may be used with data from Auger and EUSO to infer the nature of the sources of UHECRs. In §4 we discuss the possibility of using future EUSO data to measure the spectrum of a single source of cosmic rays with energy above 5×10^{19} eV. In §5 we present a critical view of the role of magnetic fields for the propagation of UHECRs, in order to define the limits of the results reported in this paper. We conclude in §6.

2 The Montecarlo simulation for cosmic ray propagation

The propagation of UHECRs is simulated here using the Montecarlo simulation described in a previous paper [3]. We refer the reader to that paper for more details, while in this section we provide the basic information.

We assume that ultra-high energy cosmic rays are protons injected with a power-law spectrum in extragalactic sources. The injection spectrum is taken to be of the form

$$F(E)dE = \alpha E^{-\gamma} \exp(-E/E_{\max})dE \quad (1)$$

where γ is the spectral index, α is a normalization constant, and E_{\max} is the maximum energy at the source.

We simulate the propagation of protons from source to observer by including

the photo-pion production, pair production, and adiabatic energy losses due to the expansion of the universe [19,3], treating photo-pion production as a discrete energy loss process.

In each step of the simulation, we calculate the pair production losses using the continuous energy loss approximation given the small inelasticity in pair production ($2m_e/m_p \simeq 10^{-3}$). For the rate of energy loss due to pair production at redshift $z = 0$, $\beta_{\text{pp}}(E, z = 0)$, we use the results from [20,21], while at redshift $z > 0$,

$$\beta_{\text{pp}}(E, z) = (1 + z)^3 \beta_{\text{pp}}((1 + z)E, z = 0). \quad (2)$$

Similarly, the rate of adiabatic energy losses due to redshift is calculated in each step using

$$\beta_{\text{rsh}}(E, z) = H_0 \left[\Omega_M (1 + z)^3 + \Omega_\Lambda \right]^{1/2}, \quad (3)$$

with $H_0 = 75 \text{ km s}^{-1} \text{ Mpc}^{-1}$.

The photo-pion production is simulated by calculating first the average number of photons able to interact via photo-pion production through the expression:

$$\langle N_{\text{ph}}(E, \Delta s) \rangle = \frac{\Delta s}{l(E, z)}, \quad (4)$$

where $l(E, z)$ is the interaction length for photo-pion production of a proton with energy E at redshift z and Δs is a step size, chosen to be much smaller than the interaction length (typically we choose $\Delta s = 100 \text{ kpc}/(1 + z)^3$).

In Fig. 1 we plot the interaction length for photopion production used in [22] (solid thin line), and in [23] (triangles). The dashed line is the result of our calculations (see below), which is in perfect agreement with the results of [22,23]. The apparent discrepancy at energies below $10^{19.5} \text{ eV}$ with the prediction of Ref. [22] is only due to the fact that we consider only microwave photons as background, while in [22] the infrared background was also considered. For our purposes, this difference is irrelevant as can be seen from the loss lengths plotted in Fig. 1. The rightmost thick solid line is the loss length for photopion production [22], while the other thick solid line is the loss length for pair production. For comparison, in Fig. 1 we also plot the loss length as calculated in [27] (thick squares). In the present calculations, we do not use the loss length of photopion production which is related to the interaction length through an angle averaged inelasticity. In our simulations we evaluate the inelastic-

ity for each single proton-photon scattering using the kinematics, rather than adopting an angle averaged value.

The interaction length is calculated as described in detail in [3]. Once the interaction length is known, we then sample a Poisson distribution with mean $\langle N_{\text{ph}}(E, \Delta s) \rangle$, to determine the actual number of photons encountered during the step Δs . When a photo-pion interaction occurs, the energy ϵ of the photon is extracted from the Planck distribution, $n_{ph}(\epsilon, T(z))$, with temperature $T(z) = T_0(1 + z)$, where $T_0 = 2.728$ K is the temperature of the cosmic microwave background at present. Since the microwave photons are isotropically distributed, the interaction angle, θ , between the proton and the photon is sampled randomly from a distribution which is flat in $\mu = \cos\theta$. Clearly only the values of ϵ and θ that generate a center of mass energy above the threshold for pion production are considered. The energy of the proton in the final state is calculated at each interaction from kinematics. The simulation is carried out until the statistics of events detected above some energy reproduces the experimental numbers. In this way we have a direct handle on the fluctuations that can be expected in the observed flux due to the stochastic nature of photo-pion production and to cosmic variance. In the presence of a homogeneous distribution of point sources the simulation proceeds in the following way: we fix the density of sources that we wish to use for the simulation and we generate at random the positions of the point sources in all the universe. For our calculations we adopt a flat Λ -dominated universe with $\Omega_\Lambda = 0.7$ and $\Omega_m = 0.3$. In a Euclidean universe, the flux from a source would scale as r^{-2} where r is the distance between the source and the observer. On the other hand, the number of sources between r and $r + dr$ would scale as r^2 , so that the probability that a given event has been generated by a source at distance r is independent of r : sources at different distances have the same probability of generating any given event. In a flat universe with a cosmological constant, this is still true provided the distance r is taken to be

$$r = c \int_{t_g}^{t_0} \frac{dt}{R(t)}, \quad (5)$$

where t_g is the age of the universe when the event was generated, t_0 is the present age of the universe, and $R(t)$ is the scale factor.

Once a source distance has been selected at random, one of the sources at that distance is picked at random and a particle energy is assigned to the event from a distribution that reflects the injection spectrum, chosen as in Eq. (1). This particle is then propagated to the observer and its energy and direction of arrival recorded. Due to the statistical error in energy determination, the recorded energy of the event is generated from a gaussian centered around the arrival energy with a spread defined by the statistical error. A

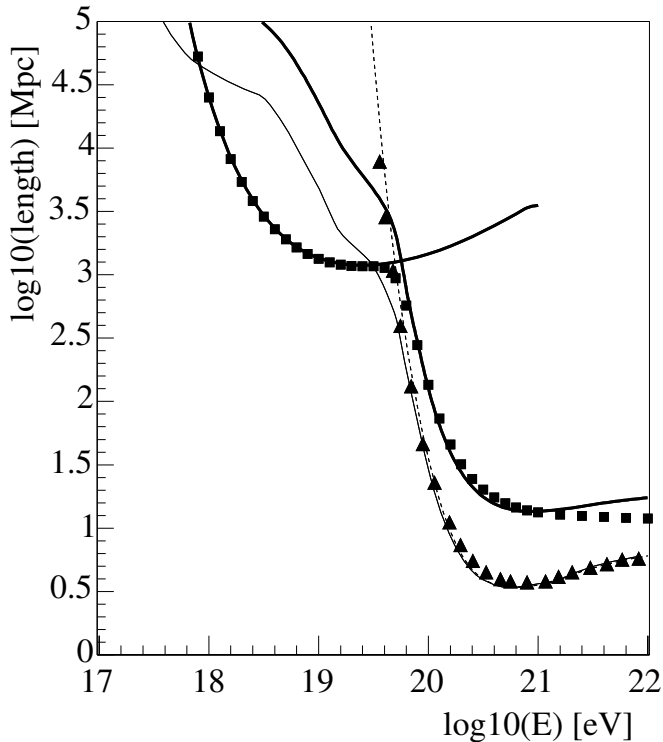


Fig. 1. Interaction length for photopion production as calculated in this paper (dashed line) compared to the interaction length of [22] (solid thin line) and of [23] (triangles). The thick solid lines are the loss lengths for photopion production (on the right) and of pair production (on the left) as obtained in [22]. The squares are the loss lengths for photopion production and proton pair production as calculated in [27].

similar procedure is adopted to account for the uncertainty in the direction of arrival, determined by the angular resolution of the instrument. This procedure is repeated until the number of events above a threshold energy, E_{th} is reproduced. With this procedure we can assess the significance of results from present experiments with limited statistics of events.

The successful results of the comparison of our findings with the results of our simulations with the analytical results [24–27] valid in the low energy regime (namely below 4×10^{19} eV) have already been discussed in [3].

3 How many sources?

In this section we illustrate the results of our calculations for the simulated number of doublets and triplets obtained using the events statistics of the

AGASA experiment with the declination dependence of the acceptance given in [28]. While the current statistics of doublets and triplets is richer, the exact arrival directions are not publically available, therefore we use here the numbers of multiplets reported in [29], for which clear information about the directions of arrival is provided. We consider several values for the source density in the local universe and two cases of source evolution with redshift, namely no evolution and evolution as $(1+z)^m$ with $m = 4$. The location of the sources is generated at random with the chosen value of the spatial density. UHECRs are then generated from these sources and propagated to the Earth as explained in §2. The angle dependence of the acceptance of the experiment is also taken into account. After generating the statistics of events observed by the experiment above some energy threshold, we calculate the number of n-plets. This procedure is repeated for 100 realizations of the source distribution in order to calculate the average expected numbers and the corresponding uncertainties.

A first information about the small and possibly large scale anisotropy of the AGASA data can be extracted from the two point correlation function of the observed data, defined as [15,17]:

$$N(\theta) = \frac{1}{S(\theta)} \sum_{i>j} R_{ij}(\theta), \quad (6)$$

where $S(\theta) = 2\pi|\cos(\theta) - \cos(\theta + \Delta\theta)|$ is the area of the angular bin between θ and $\theta + \Delta\theta$ and $R_{ij}(\theta) = 0, 1$ counts the events in the same bin.

The two point correlation function of the AGASA data is plotted as a histogram in Fig. 2 for angles between 2 and 60 degrees. In the same plot the points with error bars are the result of our simulations with the AGASA statistics of events, averaged over 100 realizations of the source distribution with a source density of 10^{-5} Mpc^{-3} (see discussion below). The presence of clusters of events reflects into the appearance of the large peak at the angular resolution of AGASA, while no additional feature is present in the two point correlation function.

We can now use our simulations to calculate the numbers of multiplets with multiplicities $n = 2, 3, \dots$ for the same energy threshold as in the AGASA experiment, namely $4 \times 10^{19} \text{ eV}$. The calculations are carried out for an opening angle of 3 degrees and an angular resolution of the AGASA experiment of 2.5 degrees. The observed spectrum of UHECRs above 10^{19} eV can be fitted equally well with an injection spectrum $E^{-2.6}$ and no redshift evolution, or with an injection spectrum $E^{-2.4}$ and redshift evolution $\propto (1+z)^4$. We carry out our simulations for both cases. The diffuse spectra that we obtain are plotted in Fig. 3 for the two cases, compared with AGASA data (thick dots).

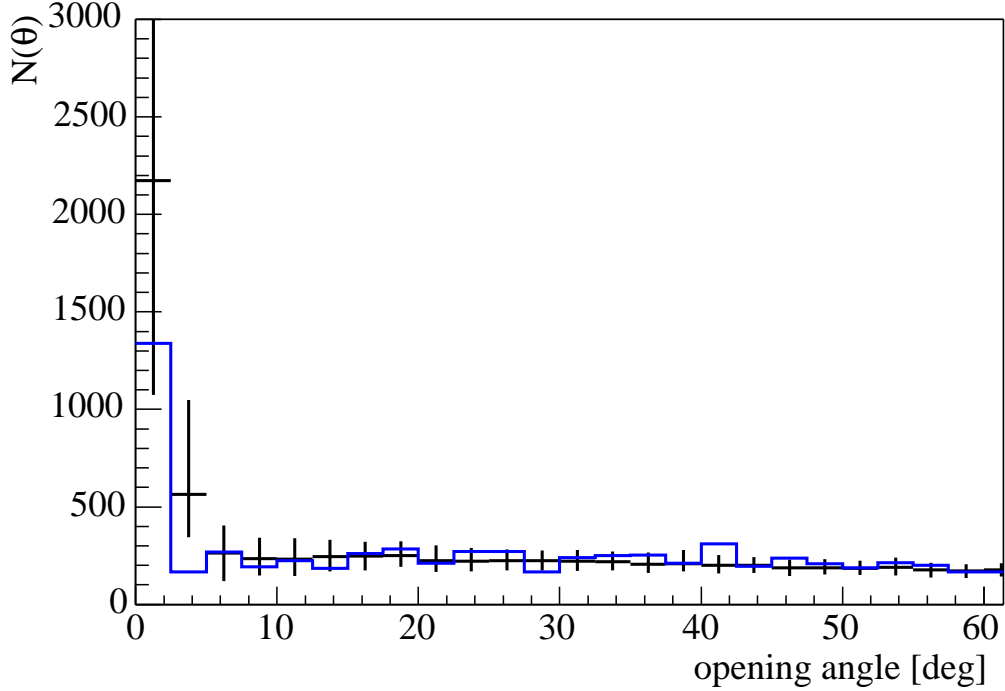


Fig. 2. Two Point correlation function of the AGASA data (histogram) compared with the prediction of our simulations (points with error bars) averaged over 100 realizations.

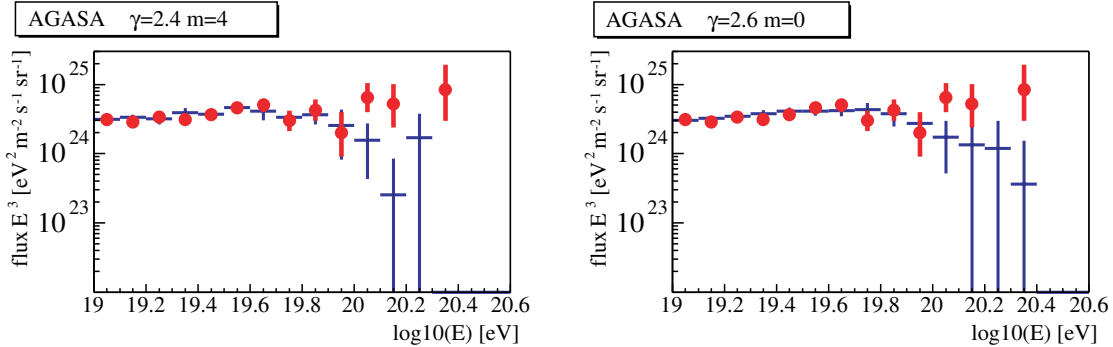


Fig. 3. Observed spectrum (thick dots with error bars) compared with the results of our calculations, using an injection spectrum $E^{-2.4}$ and redshift evolution of the sources $(1+z)^4$ (left panel) or an injection spectrum $E^{-2.6}$ with no evolution (right panel).

The calculations of the small scale anisotropies are carried out for three source densities $\rho = 10^{-6}$, $\rho = 10^{-5}$ and $\rho = 10^{-4}$ Mpc^{-3} . Our results are illustrated in Fig. 4: the plots on the left side are obtained with injection spectrum $E^{-2.6}$ and no evolution ($m = 0$), while the plots on the right are for injection spectrum $E^{-2.4}$ and $m = 4$ (strong evolution). These two cases are likely to bracket the region of plausible evolution of the sources. As we show below however, the

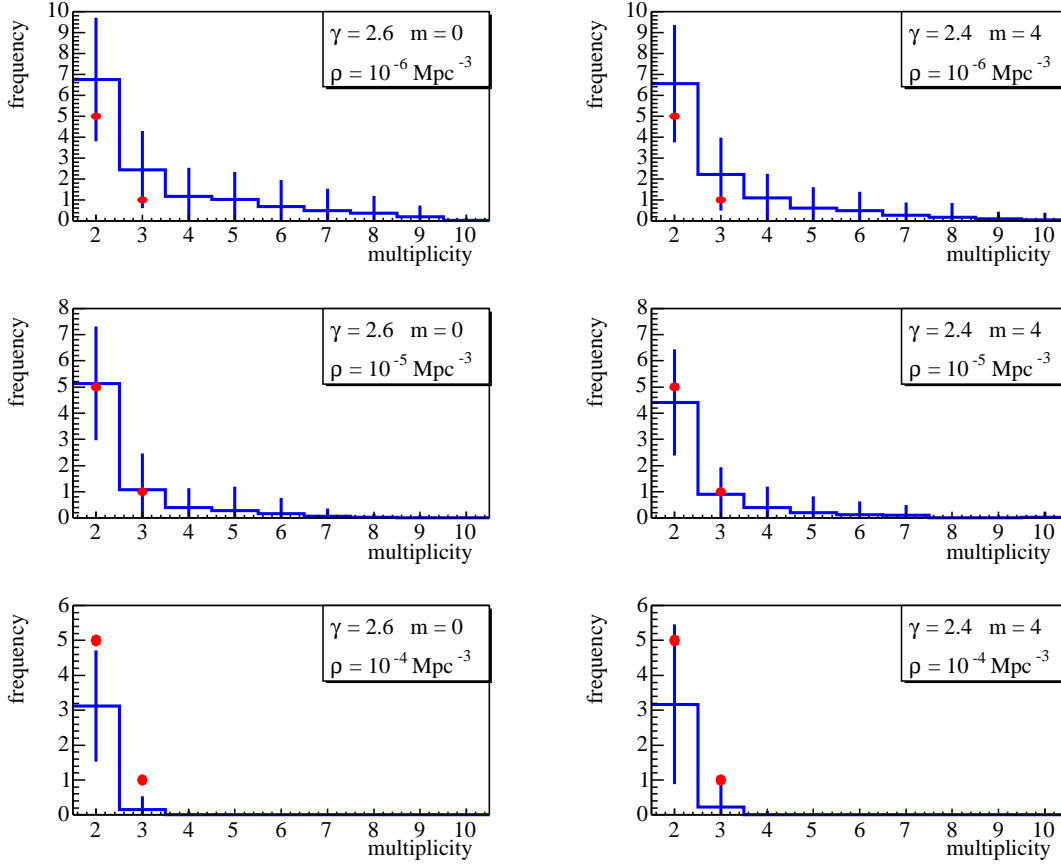


Fig. 4. Statistics of multiplets with the AGASA statistics as obtained in our simulations with the source densities indicated in the plots. The left column refers to the case without redshift evolution, while the right column refers to the case with evolution $(1+z)^4$ in the injection spectra. The dots are the AGASA findings.

evolution in the source luminosity or density does not affect in any appreciable way the small angle clustering of UHECRs. The value of the source density adopted in our calculations is indicated in the plots.

The multiplets seen by the AGASA experiment consist of 5 doublets and 1 triplet, indicated in Fig. 4 with two thick dots at multiplicities 2 and 3. For the case of low source density, $\rho = 10^{-6} \text{ Mpc}^{-3}$, there are few sources from which an event can be generated. As a consequence, the multiplets are frequent. There is a finite probability in this case to have multiplets with multiplicity up to 6, which are not observed. The case with source density $\rho = 10^{-5} \text{ Mpc}^{-3}$ provides a better description of the data, namely the numbers of doublets and triplets appear to be closer to the observed numbers and the higher multiplicity clusters are less frequent. For the higher density case, an increasing number of sources can contribute events, therefore doublets and triplets, and clearly the higher multiplicity multiplets as well, become more sparse.

We can conclude that for continuous (namely non-bursting) sources of UHE-

CRs, the expected source density should be $\rho \approx 10^{-5} \text{ Mpc}^{-3}$, with an uncertainty of more than one order of magnitude (a few - 400 sources within 100 Mpc from the Earth). The number is approximately the same for the two cases of injection spectrum and evolution. This could be expected because the sources that contribute a flux at energies above $4 \times 10^{19} \text{ eV}$ are those at redshift $z \leq 0.2 - 0.3$, where the evolution is still only marginally relevant.

It is worth stressing once more that the two point correlation function of the realizations that provide the doublets and triplets with the AGASA statistics, as shown in Fig. 2 do not show evidence for features other than the peak at small angles. In the following we consider the situation that we expect to take place for Auger and EUSO.

The case of the Auger Observatory

We consider here the Auger observatory in the south emisphere, with total acceptance of $7000 \text{ km}^2 \text{ sr}$, and declination dependence as given in [30]. This number has to be compared with the AGASA acceptance of $160 \text{ km}^2 \text{ sr}$. AGASA has detected 886 events above 10^{19} eV , with an exposure of $1645 \text{ km}^2 \text{ sr yr}$. In 5 years of operation of Auger, this would correspond to $\sim 1.9 \times 10^4$ events above 10^{19} eV and 1.5×10^3 events above $4 \times 10^{19} \text{ eV}$. The expected number of events above 10^{20} eV is more dependent on details of the cosmic ray propagation. For an injection spectrum $E^{-2.6}$ and with no luminosity evolution of the sources, we predict $\sim 60 - 70$ events with energy above 10^{20} eV . About 10% of the events are expected to be detected by both the ground array and the fluorescence telescopes.

In Fig. 5 we plot the two point correlation function obtained for Auger above 10^{19} eV (left upper plot) and above $4 \times 10^{19} \text{ eV}$ (right upper plot) with 2 degrees angular resolution, and using a source density of 10^{-5} Mpc^{-3} . The lower plots represent one realization of the sky in the same energy region as in the corresponding upper plot (the realization provides the numbers of doublets and triplets currently seen by AGASA. The solid line identifies the supergalactic plane while the dashed line locates the galactic plane). Again, no feature is present in the two point correlation function with the exception of the peak at small angles.

Although these plots refer to a specific realization, it can be shown that the correlation function averaged over many realizations has a similar shape and the same peak at small angles, but with large error bars. The reason for these uncertainties is that with the expected number of events above $4 \times 10^{19} \text{ eV}$ (~ 1500), the angular distance between two events in the sky is ~ 2 degrees, comparable with the point spread function of the experiment. In these circumstances the accidental clusters of events, namely those that are not associated with a point source, are very frequent. In this respect the correlation

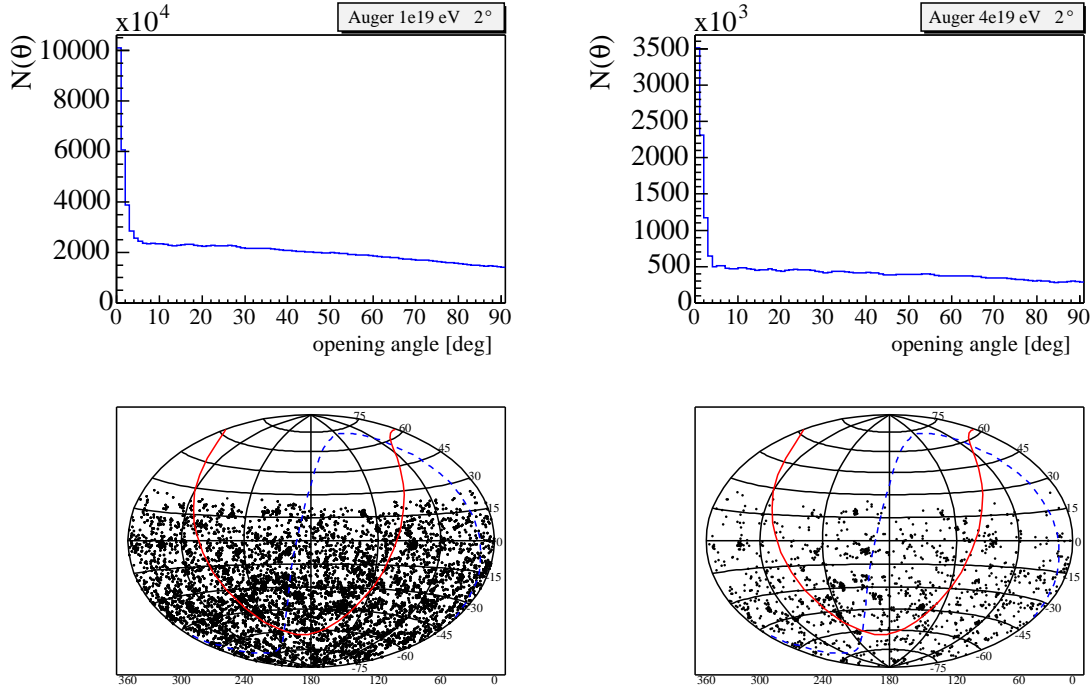


Fig. 5. Upper plots: two point correlation function for the Auger expected statistics above 10^{19} eV (on the left) and above 4×10^{19} eV (on the right). The lower plots are the corresponding sky maps for one realization of the source distribution.

function of the events above 4×10^{19} eV might not be the best tool to count the sources of UHECRs. We make the attempt to apply the same method restricted to events above 10^{20} eV. Our results for the two point correlation function are plotted in Fig. 6 for three values of the source density, namely 10^{-6} , 10^{-5} and 10^{-4} Mpc^{-3} . The error bars are obtained after averaging the propagation over 100 realizations of the source distribution. On the basis of the size of the error bars, it appears that it should be reasonably simple with Auger data above 10^{20} eV to infer the source density within at least one order of magnitude, which is a clear improvement on what is possible to achieve with AGASA data.

In Fig. 7 we plot the average number of clusters of events with different multiplicity and related error bars, as expected above 10^{20} eV in Auger, for the three values of the density of sources. The error bar in the number of doublets appears to be small enough to allow one to determine the number of sources by following the same procedure illustrated above for the case of AGASA. Note that here the multiplets are counted in a *non compact* manner, namely a set of N events qualifies as a N -plet even if not all the pairs of events within it have an angular separation less than some value which is fixed in the analysis. This creates some ambiguity in the definition of a cluster, but more rigorous definitions can be easily found. We adopted this definition in order to avoid

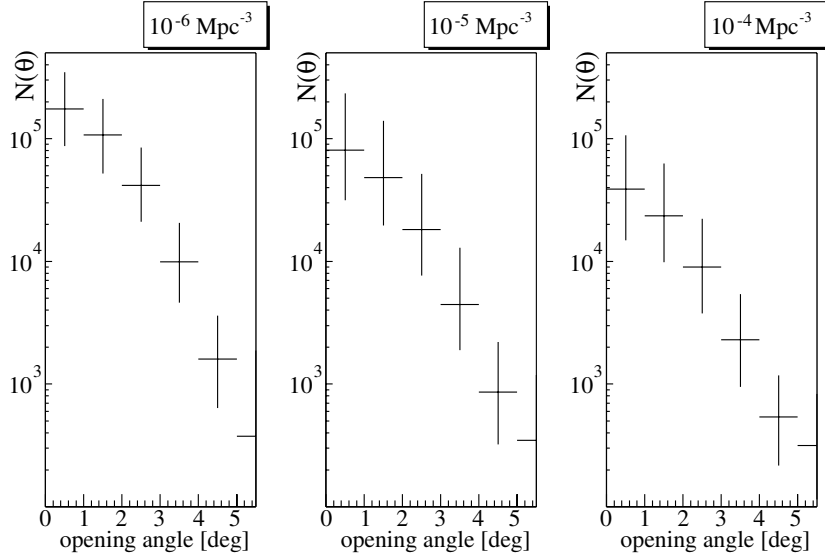


Fig. 6. Two Point correlation function for the Auger simulated data above 10^{20} eV for source density 10^{-6} , 10^{-5} and 10^{-4} Mpc^{-3} .

to check the angular distances of all the pairs of events in a multiplet with very high multiplicity, since this can easily become an unfeasible task for large values of N .

It is worth noticing that the tendency here is the opposite with respect to that obtained for the AGASA statistics: the number of doublets increases with increasing source density. At first this may seem counterintuitive, because with a larger number of sources to generate an event from, it is likely that each time a different source is picked. On the other hand, when the number of events ($\sim 60 - 70$ for Auger above 10^{20} eV) becomes comparable with the number of sources that can contribute the events, the clustering becomes more probable and higher multiplicity clusters appear. This reflects in the fact that the ratio of the number of events that come in singlets to the number of clustered events increases when the source density increases.

The case of EUSO

The EUSO acceptance is known within a factor of ~ 2 and amounts to $35000 - 70000 \text{ km}^2 \text{ sr}$. The observation time is supposed to be 3 years, therefore the total exposure is expected to be of $\sim (1 - 2) \times 10^5 \text{ km}^2 \text{ sr yr}$. If the GZK feature is in fact present in the cosmic ray data, the expected number of events above 10^{20} eV in EUSO is $\sim 180 - 360$ if the maximum energy of the particles at the sources is large enough.

In the following we consider two cases for the EUSO acceptance, with average number of events above 10^{20} eV equal to 180 (low acceptance case) and 360 (high acceptance case). The correlation function for the low (left upper plot)

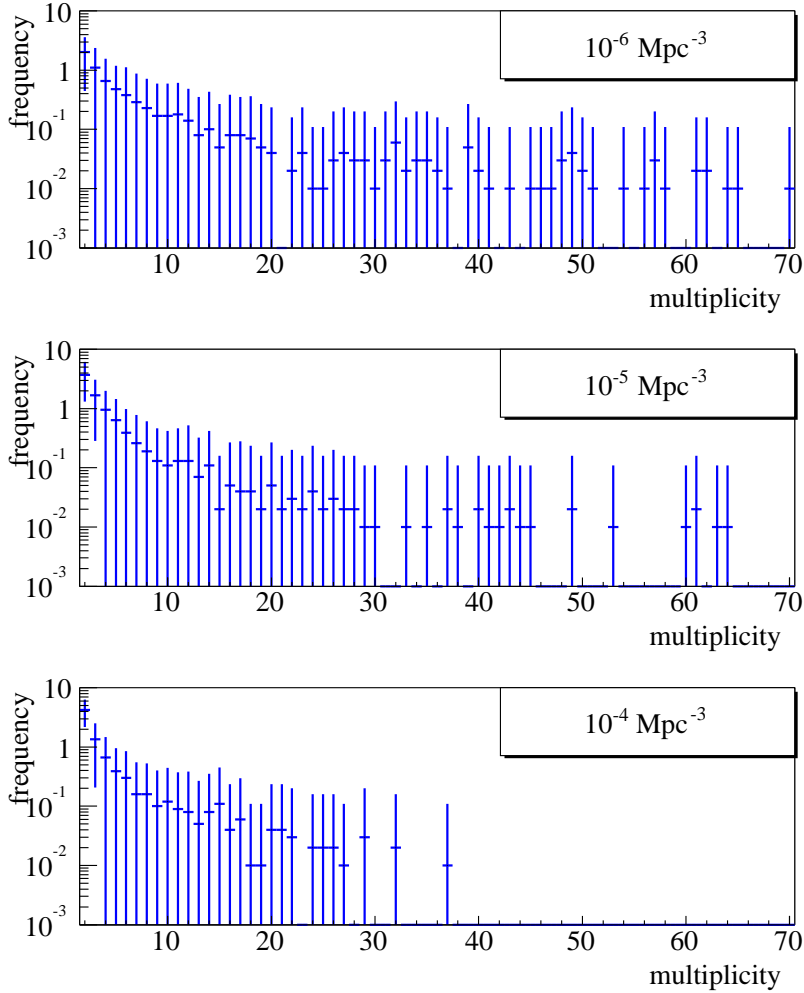


Fig. 7. Multiplets of events in the Auger simulated data above 10^{20} eV for source density 10^{-6} , 10^{-5} and 10^{-4} Mpc^{-3} .

and high acceptance (right upper plot) cases is plotted in Fig. 8 for a density of sources 10^{-5}Mpc^{-3} . The corresponding sky is illustrated in the lower plots in Fig. 8.

In the large angle region, where no feature was found for the AGASA and Auger statistics of events, the simulated data for the EUSO experiment show evidence for some wiggles around the average value of the two point correlation function at large angles, that is $\sim N_{ev}^2/8\pi$, where N_{ev} is the number of events used for the analysis. The error bars are calculated by generating 100 realizations of the propagation of UHECRs, at fixed configuration of the sources and at fixed number of events above some threshold. The size of the error bars shows that these features should be visible in the two point correlation function even after accounting for uncertainties in the particle propagation. In other words, the peaks are not due to limited statistics of events in the energy region of interest. A similar plot for the Auger expected number of events

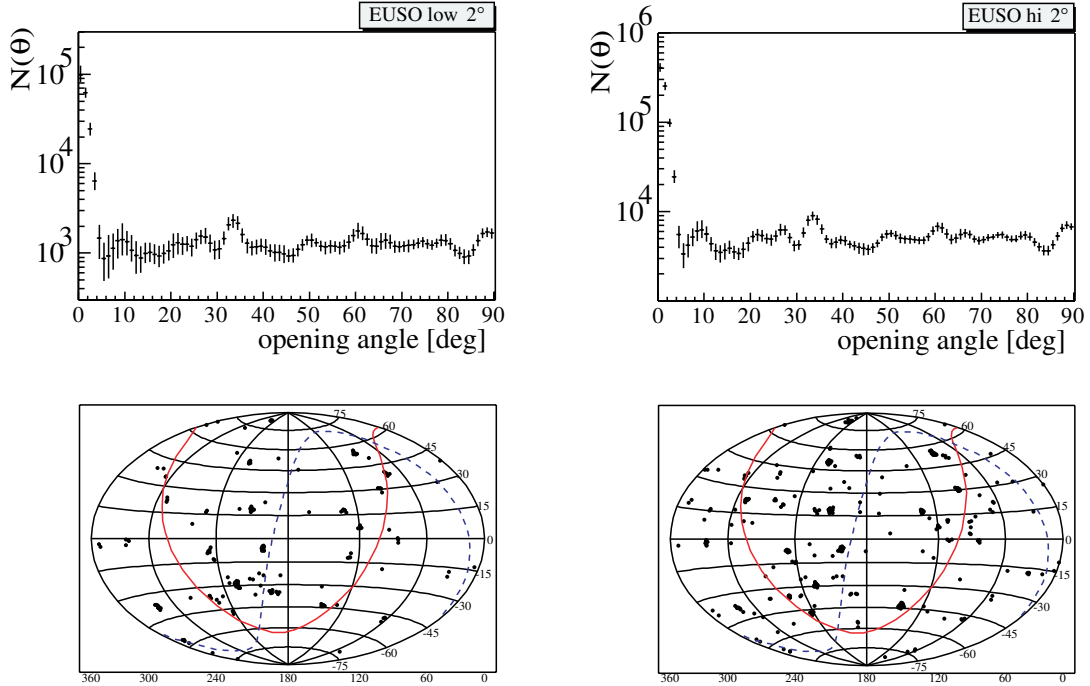


Fig. 8. Upper plots: two point correlation function for the EUSO expected statistics above 10^{20} eV for its baseline configuration (left) and twice as much (right). The lower plots are the corresponding sky maps for one realization of the source distribution.

above 10^{20} eV shows error bars which hide almost completely the wiggles in the correlation function.

The wiggles are the consequence of random noise in the source distribution: this can be understood in terms of fluctuation of the number of sources that may contribute events in the angular bin between θ and $\theta + \Delta\theta$. According with this interpretation, one expects that the amplitude of these fluctuations gets larger for lower source densities. Note that we are calculating the two point correlation function of the events and not of the sources, therefore the information on the sources is embedded in the two point correlation function and needs to be disentangled from the information on the events. On the other hand, with the EUSO statistics of events the fluctuations due to the propagation have been shown to be irrelevant, therefore the remaining fluctuations have to be due to the random distribution of the sources. The question we address here is whether we can use the amplitude of the fluctuations around the average of the two point correlation function as an indicator of the density of sources. In Fig. 9 we plot the two point correlation function for three values of the source density, namely $\rho = 10^{-6}$, $\rho = 10^{-5}$ and $\rho = 10^{-4}$ Mpc^{-3} averaged over 2200 realizations of the source distribution. One can clearly see that the scatter in the large angles part of the two point correlation function around

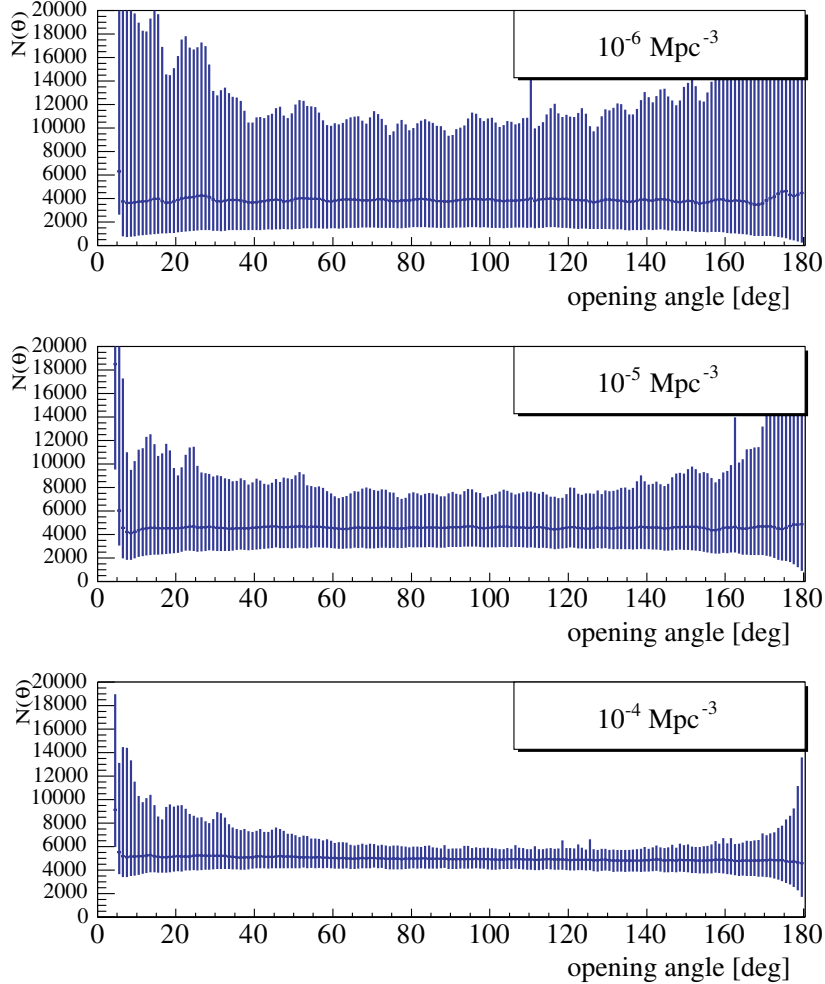


Fig. 9. Two point correlation function for the EUSO statistics of events above 10^{20} eV, in the high acceptance case. The density of sources is as indicated in the panels. The error bars are obtained by averaging the correlation function on 2200 realizations of the source distribution.

its average value are much larger for the low density case than for the higher density cases, as expected. One can calculate for each realization of the sources the average variance of the two point correlation function around the expected average at angles between 20 and 160 degrees and then plot the distribution of variances, for the three values of the source density. This graph is shown in Fig. 10 for 2200 realizations of the source distribution. As an instance, the realization used to obtain Fig. 8 (source density 10^{-5} Mpc^{-3}) had average variance around the mean equal to 1200. This value is just on the right of the peak of the distribution of variances for a source density 10^{-4} Mpc^{-3} and on the immediate left of the peak for source density 10^{-5} Mpc^{-3} . The probability to get a larger (smaller) variance in the two cases respectively is 28% (20%). The value of the variance in our specific realization is on the very tail of the distribution for 10^{-6} Mpc^{-3} , with a probability of getting less of only 2%.

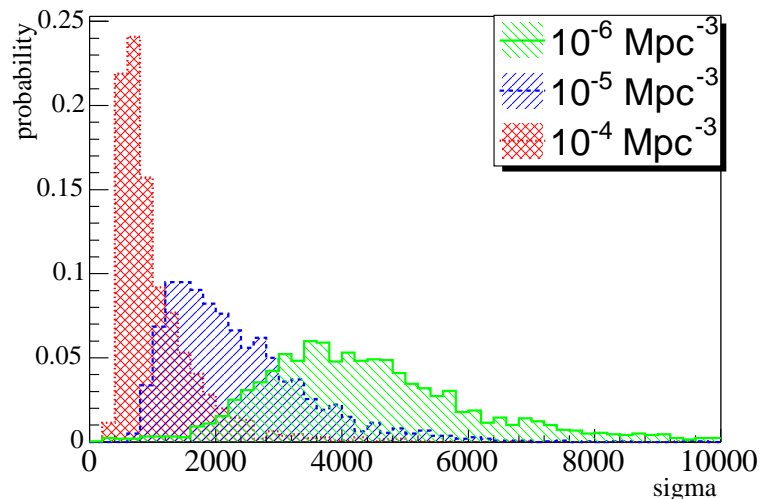


Fig. 10. Distribution of the variances around the mean of the two point correlation function for the three values of the source density, as indicated. The histograms are obtained by averaging over 2200 realizations of the source distribution.

The appearance of the wiggles in the two point correlation function is the result of an interesting effect, peculiar of the ultra high energy cosmic rays with energy above 10^{20} eV. The point-like nature of the sources arises in the two point correlation function when the number of events equals or exceeds the number of sources that can contribute events in the energy region of interest. For instance, for the AGASA data above 4×10^{19} eV the number of events is a few tens but the sources that can contribute are all the sources within ~ 1000 Mpc. For the densities that we found, the number of events is always much smaller than the number of sources that generate them. In other words most sources did not contribute any events at the detector. For Auger, we expect ~ 1500 events at energies above 4×10^{19} eV, while the sources that may contribute are 2×10^4 for source density 10^{-5} Mpc^{-3} (Auger sees about half of the sky) which is always larger than the number of events for the three source densities that we restricted our attention to. Moreover, even from a visual look at the sky as simulated for the Auger statistics, Fig. 5, the point-like nature of the sources is not very evident.

A benchmark estimate can help understand the effect: the number of events detected by an experiment with exposure Σ_{exp} (in units of $\text{km}^2 \text{ sr yr}$) above some energy threshold E_{min} can be written as

$$\begin{aligned}
 N_{ev}(E > E_{th}) &= \Sigma_{exp} \frac{1}{4\pi} \int_{E_{min}} dE \int_0^{R(E)} dr \rho 4\pi r^2 \frac{\Phi(E)}{4\pi r^2} \approx \\
 &\approx \Sigma_{exp} \frac{\rho}{4\pi} \Phi(E_{min}) E_{min} R(E_{min}) , \tag{7}
 \end{aligned}$$

where $R(E)$ is the range of cosmic rays with energy E and $\Phi(E)dE$ is the number of particles injected by the source in the energy range between E and $E + dE$.

For the AGASA experiment, adopting a threshold $E_{min} = 4 \times 10^{19}$ eV, one has $\Sigma_{exp} = 1645$ km² sr yr, $N_{ev}(E > E_{th}) = 72$ and $R_{min} \approx 1000$ Mpc. We have already found that the observed doublets and triplets hint at a source density $\sim 10^{-5}$ Mpc⁻³. Let us denote in general the source density as $\rho = 10^{-5}\rho_{-5}$ Mpc⁻³. It is therefore easy to use the previous expression to obtain

$$\Phi(E_{min}) \approx 1.3 \times 10^{21} \rho_{-5} \text{ eV}^{-1} \text{ yr}^{-1},$$

consistent with an injection of $\sim 10^{42}$ erg s⁻¹ per source in the energy range $E > 10^{19}$ eV, found with more detailed calculations.

Using now Eq. (7) one can estimate which exposure is needed at energies above 10^{20} eV, in order to make sure that we receive at least one event per source on average, namely that each source has contributed at least one event at the detector. Putting numbers in the equation above, and adopting $R(10^{20} \text{ eV}) \approx 100$ Mpc, and an injection spectrum $E^{-2.6}$, we easily obtain the condition

$$\Sigma_{exp} > \Sigma_c = 42000 \rho_{-5} \text{ km}^2 \text{ sr yr}. \quad (8)$$

The critical exposure Σ_c should be compared with $\Sigma_{Auger} = 35000$ km² sr yr of Auger after 5 years of operation, and with $\Sigma_{EUSO} \sim 10^5$ km² sr yr after 3 years of operation of EUSO. If one interprets our analysis in Fig. 4 as evidence that the most likely range of source densities should be $10^{-5} - 10^{-4}$ Mpc⁻³, then EUSO is expected to have exposure above the critical. Auger is above the critical exposure only for the lower limit on the source density, $\rho = 10^{-6}$ Mpc⁻³.

Rephrasing this result, with an experiment with sufficiently large exposure, at energies above 10^{20} eV each source has statistically contributed at least one of the detected events. Further increase in the experimental exposure at energies above 10^{20} eV would not increase the number of fainter (more distant) sources, but should rather imply an increase in the number of events received from each source within the maximum distance from which the events can reach the Earth. This is a direct consequence of the physical meaning of the GZK feature in the cosmic ray spectrum, and is of crucial importance for the evaluation of the number of sources of UHECRs in the universe. In fact, the number of sources can be simply obtained by counting the multiplets (with multiplicity 1, 2, 3, ...) in the observed data. This approach is hardly applicable at lower energies: particles with energy 4×10^{19} eV may reach the Earth from 1 Gpc distance, so that the identification of multiplets may in fact be problematic.

We implemented a routine for the identification of the clusters of events and

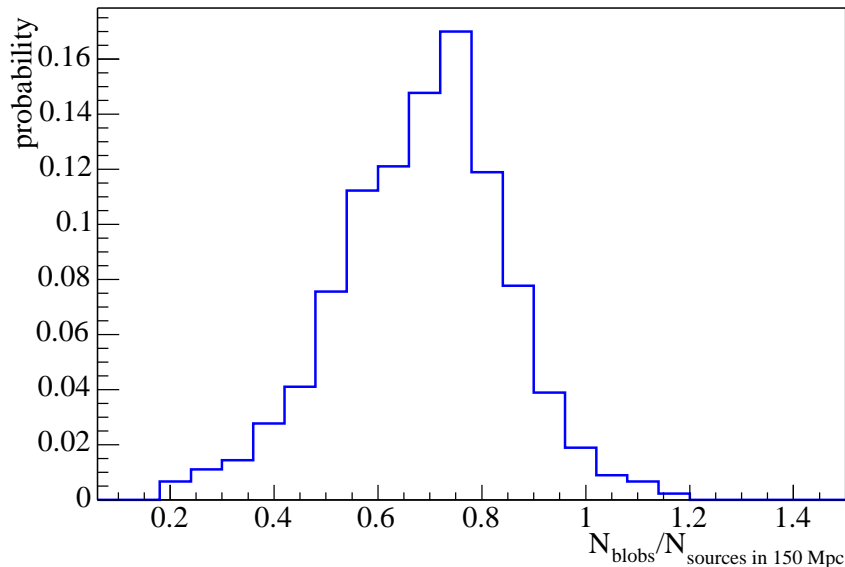


Fig. 11. Results of the source counting procedure based on the identification of clusters of events in the sky. On the x-axis the ratio of the number of sources counted through the clusters and the *real* number of sources within 150 Mpc is plotted.

the counting procedure generates the correct number of sources within $L_{95} = 150$ Mpc, as illustrated in Fig. 11, where we plot the ratio of the number of sources obtained from the counting procedure and the *real* number of sources in the simulation. Typically $\sim 70-80\%$ of the sources are correctly counted. This uncertainty should be compared with the 1-2 orders of magnitude uncertainty that can be achieved from current data on the small scale clustering. The distance $L_{95} = 150$ Mpc has been evaluated numerically and represents the distance from which 95% of the events with detected energy above 10^{20} eV start. We stress that the detected energy is affected by a statistical error of $\sim 30\%$ that needs to be accounted for, when evaluating the distance L_{95} .

4 Direct measurement of a source distance, spectrum and intrinsic luminosity

The large statistics of events that will likely be available with future UHECR observatories will provide us with the unique opportunity to see a single source directly and have information about its injection spectrum, distance and luminosity. As discussed in the previous section, several point sources are expected to appear in EUSO as multiplets with multiplicity $\sim 20-70$ at energies above 10^{20} eV. This implies that the spectrum of UHECRs from those sources can be reconstructed to some extent. If the threshold for triggering of events in

EUSO is lowered to 5×19^{19} , even if with some efficiency factor, this would make the spectral reconstruction even more powerful. For the Auger telescope these conditions are supposed to be less probable, but it may happen that there is a nearby powerful source for which the analysis can be carried out.

It is worth recalling that the GZK feature in the spectrum of single sources appears to be much more pronounced than in the diffuse flux, since the latter derives from the superposition of the contributions of the spectra of many sources with the GZK feature at different energies. Therefore, studying the spectra of isolated sources it is possible in principle to infer the injection spectrum and/or the distance to the source. A practical example is provided here, in which we use the events that are associated in Fig. 8 with the higher multiplicity cluster of events in the realization, identified as a source. Note that in this realization, the cluster only contained 20 events at energies larger than 10^{20} eV. This is one of the most pessimistic situations, since in many realizations clusters containing up to 70 events are found. In Fig. 12 we plot the spectrum of the events above 5×10^{19} eV coming from the cluster (thick dots with error bars) together with four mock (simulated) spectra from sources with the same events statistics at four different distances (10, 20, 50, 100 Mpc). The simulated (mock) spectra from the source are averaged over many realizations in order to estimate the error bars due to fluctuations in photopion production. For a source at 10Mpc we predict a larger number of events at high energies (assuming that the maximum energy at the source is large enough). A fit by eye would suggest that the most likely distance to the source would be 50 – 100 Mpc. Moreover, for a total of 120 events above 5×10^{19} eV (observed) one would expect that above 10^{20} eV the events would be 35 ± 6 for a distance of 10 Mpc, 32 ± 5 for a source at 20 Mpc, 21 ± 5 for a source distance of 50 Mpc and 10 ± 3 for a source distance of 100 Mpc, to be compared with the observed 22 events in the cluster of events identified as a source, which in the simulation sits at 48 Mpc. The identification of ~ 50 Mpc as the likely distance of the source seems to be rather easy to achieve.

It is important to stress that while the current data allow one to speculate that the lack of association of the Fly’s Eye event at 3×10^{20} eV with any kind of source within 30 Mpc may be due to some unknown carrier, insensitive to the photopion production energy losses, the measurement of the spectrum of the source should pin down the source distance, independently of its direct identification at other wavelengths.

5 The role of the Intergalactic Magnetic Field

Much debate exists in current literature about the role of intergalactic magnetic fields upon the propagation of UHECRs from their sources to the Earth.

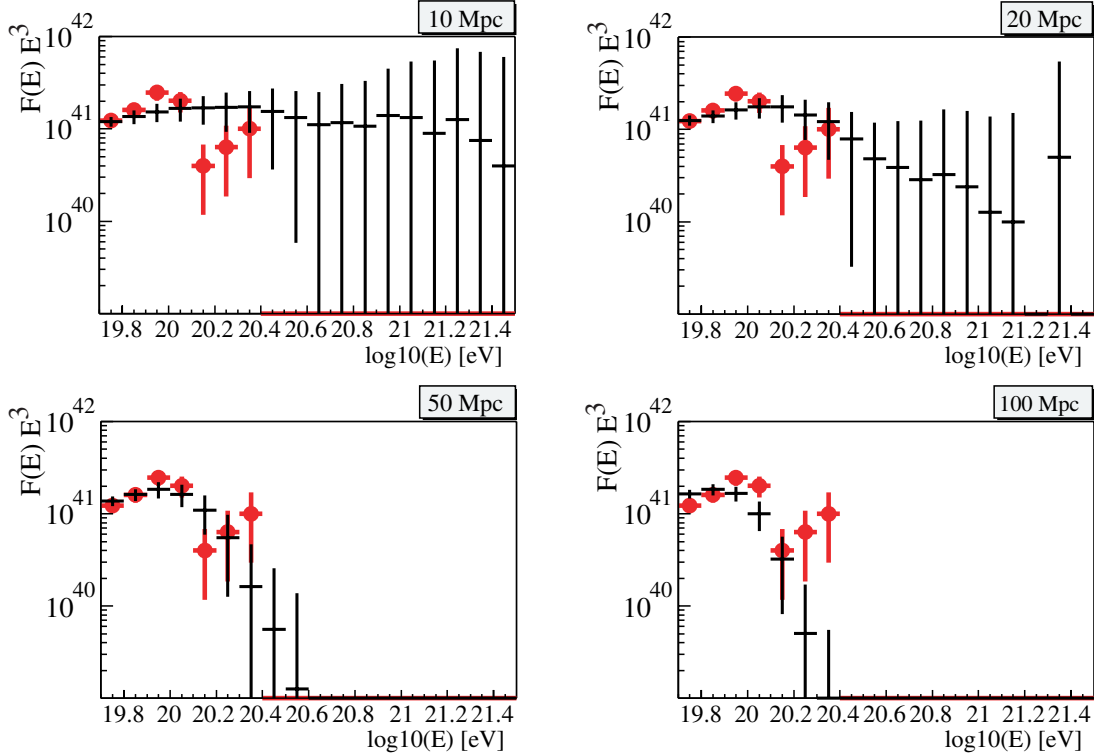


Fig. 12. Spectrum of a cluster of events (thick dots with error bars) and the spectra of sources at distances 10, 20, 50 100 Mpc with the same number of events (arbitrary units).

This is a debate hard to settle since our knowledge of extragalactic magnetic field strength and structure is very poor. We have a few pieces of information which are however difficult to fit in a single puzzle. In this section we briefly summarize these pieces of information and we make the attempt to establish the boundaries of the region of applicability of the results presented in this paper.

The strongest limits on the intergalactic average magnetic field presently come from measurements of the Faraday rotation of distant sources. As found in [31], the limits are at the level of 10^{-9} Gauss for a coherence length of 50 Mpc, but it is worth to keep in mind that the large fluctuations found in [31] make this limit very uncertain.

There is at present no evidences that there are magnetic fields in the intergalactic medium outside large scale structures, such as galaxies and clusters of galaxies. In galaxies there are plenty of measurements of magnetic fields. In particular, in our own galaxy the magnetic field appears to be in rough equipartition with the thermal and cosmic ray content. Galactic magnetic fields are however hardly of any relevance for the propagation of cosmic ray protons with energy above 4×10^{19} eV: the Larmor radius of these particles is in fact much larger than the size of a Galaxy and moreover the volume filling

factor of the universe in the form of galaxies is extremely small, roughly 10^{-5} .

In clusters of galaxies, there are two separate avenues through which magnetic fields have been inferred, namely through measurements of the Faraday rotation of intracluster sources, and from observation of nonthermal radio and hard X-ray emissions. Radio emission is the result of synchrotron emission of relativistic electrons in the intracluster magnetic field, while the hard X-ray emission, observed only from a few clusters of galaxies, has a more uncertain interpretation. However, the most straightforward explanation for the X radiation is that it is the result of Inverse Compton Scattering (ICS) of the same electrons responsible for the diffuse radio emission against the photons of the cosmic microwave background. If this is the right interpretation, then the magnetic field in the intracluster medium of a few clusters can be inferred to be in the range $0.1 - 1\mu G$. Several avenues have been proposed to avoid the apparent discrepancy between these values and those measured through Faraday rotation, which are typically larger [34]. The latter in particular depend upon the electron density along the line of sight, relatively well known from observations of the thermal X radiation, and the coherence length of the field, which is unknown.

Note that the thermal energy density in a cluster of galaxies is

$$E_{th} = (3/2)n_{gas}kT \approx 2 \times 10^{-11} \frac{n_{gas}}{10^{-3} \text{ cm}^{-3}} \frac{T}{10^8 \text{ K}} \text{erg cm}^{-3},$$

to be compared with the magnetic energy density $E_B = B^2/8\pi = 4 \times 10^{-14}(B/\mu G)^2 \text{ erg cm}^{-3}$, about 500 times less than the thermal energy density, despite the fact that clusters of galaxies are virialized objects.

Magnetic fields with strength of μG over a Mpc scale do affect the propagation of UHECRs. However, clusters of galaxies fill about 10^{-5} of the volume of the universe, therefore it is very unlikely that they can appreciably modify the spectra of diffuse UHECRs received at the Earth.

From the discussion above, we conclude that the only magnetic fields that can affect the propagation of UHECRs are the intergalactic fields outside galaxies and clusters of galaxies. For the sake of clarity, let us split the discussion in two parts, one concerning the magnetic field in the intergalactic space on large scales, and the other concerning our cosmic neighborhood, the so-called local supercluster (LSC).

On the large scales which are of relevance for the propagation of UHECRs with energy below 4×10^{19} eV, the limits on the magnetic field are as described above and depend upon the reversal scale of the field L_c . The results presented here remain valid as long as the angular deflection during the propagation along a path of length D stays smaller than the angular resolution of an experiment

θ_{exp} . In other words, the following condition has to be fulfilled:

$$B < 10^{-10} \left(\frac{E}{4 \times 10^{19} \text{eV}} \right) \left(\frac{\theta_{exp}}{2^\circ} \right) \left(\frac{D}{1000 \text{Mpc}} \right)^{-1/2} \left(\frac{L_c}{1 \text{Mpc}} \right)^{-1/2} \text{ Gauss.}$$

Clearly the most severe constraints concern the case of AGASA where in order to collect enough statistics of events one has to consider particles with energy above 4×10^{19} eV, whose loss length is ~ 1000 Mpc. In this case, our results are valid if the magnetic field is smaller than 1.3×10^{-10} Gauss, if $L_c = 1 \text{Mpc}$ and $\theta_{exp} = 2.5^\circ$. Whether this is a reasonable value for L_c is debatable since it depends crucially on the model for the magnetic field in the intergalactic medium. If the field is of cosmological origin, then $L_c = 1 \text{Mpc}$ may be a reasonable assumption. On the other hand, if the intergalactic medium is polluted by the magnetic field spilled out of galaxies through winds, a more reasonable value would be $L_c \sim 100$ kpc. In this case however it is misleading to think of the universe as filled by a homogeneous magnetic field with some coherence length. It is probably more correct to picture it in terms of magnetized bubbles with relatively strong magnetic fields surrounded by regions where there is no field [33]. In any case, if we take $L_c = 100$ kpc, then our analysis remains valid at least for $B < 4 \times 10^{-10}$ Gauss, and this is probably a too strong constraint. These values are in the same region of magnetic fields constrained by Faraday rotation measurements, which leads us to believe that our results may be considered sufficiently general.

We consider now our cosmic neighborhood and we address the issue of whether strong fields can be present there. The only evidence for magnetic fields in superclusters comes from observations of a tenuous diffuse radio emission from a *bridge* connecting the Coma cluster with Abell 1367, detected at 360 MHz [32]. The two clusters are ~ 40 Mpc away from each other, but it is important to stress that the so-called bridge extends only for $1.4 h_{75}^{-1}$ Mpc out of the core of the Coma cluster, whose virial radius is ~ 3 Mpc (here h_{75} is the Hubble constant in units of $75 \text{Km s}^{-1} \text{Mpc}^{-1}$). The radio emission is a clear indication of the presence of a magnetic field, but by itself cannot provide the value of this field, since the same radio flux can be achieved by changing both the magnetic field and the electron density. An assumption which is often made in Radio Astronomy is to assume that the magnetic field is in equipartition with the relativistic electrons and protons in the medium, the ratio of the two being completely unknown. If one accepts this assumption, and if a guess about the ratio of electrons to protons is made (in [32] this ratio is taken equal to unity) and assuming a spectrum for the radiating electrons, the authors derive a magnetic field of $\sim 0.6 \mu G$. Aside from the many assumptions that need to be used to derive this result, it should be kept in mind that the bridge extends over regions of space which are much smaller than the distance between Coma and A1367 and in fact smaller than the virial radius of Coma. From the point of view of the propagation of UHECRs in superclusters this is hardly an evidence

for μG magnetic fields in particular if extended to all superclusters.

The local supercluster is a ~ 40 Mpc long elongated structure with the Virgo cluster of galaxies in its center and the local group (with our Galaxy in it) at its edge. Its average overdensity is ~ 2 , typical of large scale structures that have not reached yet the virial equilibrium. Aside from the region around M87, a radio galaxy in the center of the Virgo cluster, there is no other evidence for magnetic fields in the LSC. In the likely assumption that the supercluster is not a magnetically dominated structure, namely that the energy density in the field is smaller than the thermal energy density, the condition $B \ll 0.1\mu G$ on the magnetic field must hold. Here we assumed that the baryon density is twice that in the background and that the temperature in the supercluster is $\sim 10^6$ K.

The propagation of cosmic rays with energy above 4×10^{19} eV would certainly be affected by magnetic fields of the order of $10^{-2} - 10^{-1}\mu G$ in the LSC. On the other hand one should keep in mind an important fact which is often ignored in Montecarlo calculations of the propagation in strong local fields, namely that the flux of CRs at energies below 4×10^{19} eV can reach the Earth from cosmological distances. UHECRs in the energy range around 4×10^{19} eV have a loss length comparable with the size of the universe, say 1 Gpc. If $j_{CR}(E)$ is the cosmic ray emissivity in the intergalactic space, the corresponding emissivity in the LSC will be in general amplified by some factor $\xi > 1$. The flux of UHECRs contributed by the LSC is therefore $\Phi_{LSC} \sim \xi j_{CR} R_{SLC}$ if the field is not large enough to fall in the diffusive regime of cosmic ray propagation. The flux contributed by the rest of the universe is however $\sim j_{CR} L_{loss}$ (with L_{loss} the loss length), so that the ratio of the two is $\sim 10^{-2} \xi$ at energies $\sim 4 \times 10^{19}$ eV. As stressed above, the local overdensity in the LSC is ~ 2 , therefore we expect ξ to be of the same order. It follows that the flux of UHECRs at the Earth at energies $\sim 4 \times 10^{19}$ eV is dominated by the universe outside the LSC. It is therefore necessary to simulate the propagation of UHECRs over the whole universe for the purpose of understanding spectrum and anisotropies of cosmic rays around $\sim 4 \times 10^{19}$ eV. The numerical investigations in [17] concerning the small scale anisotropies from sources in the LSC and in [18], that make an attempt to adopt a realistic local structure of the magnetic field and sources, do not include this important effect.

We summarize the discussion above as follows:

1) the magnetic field in the universe is likely to have a bubble-like structure, with regions in which the field is relatively intense, surrounded by large volumes where the magnetic pollution is not present. If the magnetic field is of cosmological origin, the region of values of the average magnetic field for which the analysis presented here can be applied overlaps with the upper limits obtained from Faraday rotation measures. If the correlation, claimed in [1],

between UHECRs (with energy between 2×10^{19} eV and 10^{20} eV) and distant BL Lac objects is correct, then a clear evidence of very weak magnetic fields over cosmological scales follows [33].

2) A magnetic field as strong as $\sim 10^{-8}$ Gauss (equal to the equipartition field) in the LSC would still be consistent with upper limits derived from measurements of Faraday rotation. However at present there is no indication or evidence that such a magnetic field is in fact there. Moreover, as found in [14,15], such a field may be hard to reconcile with the multiplets observed with AGASA. It is therefore important to understand which information can be inferred from small scale anisotropies of UHECRs in the simplest possible scenario, namely in the regime of weak fields. We will consider some implications of a possible weak local magnetic field in a forthcoming paper, since as is well known, cosmic rays remain a precious tool to investigate the presence of magnetic fields in the universe.

6 Discussion and Conclusions

We investigated the potential of present and future experiments to identify the sources of UHECRs, by using the combined information on the spectrum and small scale anisotropies in the arrival directions.

While the spectrum of UHECRs can be used to obtain the total rate of energy injection per unit volume, corresponding to $\sim 6 \times 10^{44}$ erg yr $^{-1}$ Mpc $^{-3}$ above 10^{19} eV, the existence of small scale anisotropies in the AGASA data allows us to infer the approximate density of sources, with an approximation of less than two orders of magnitude around the average value of $\sim 10^{-5}$ Mpc $^{-3}$. The luminosity per source is therefore $L_{source} \approx 2 \times 10^{42}$ erg s $^{-1}$ above 10^{19} eV, for a best fit injection spectrum $E^{-2.6}$. If extrapolated to lower energies, the corresponding luminosity increases to $L_{source} \approx 2 \times 10^{48}$ erg s $^{-1}$ above 1 GeV. This number suggests that the sources should in fact be very bright, unless a mechanism is found to limit the acceleration only to very high energy particles: for instance, for the case of acceleration at relativistic shocks moving with Lorentz factor Γ_{sh} , a minimum energy of $\Gamma_{sh}^2 m_p c^2$ is expected, which may decrease the required luminosity appreciably.

In case of evolution of the sources with a functional dependence $(1+z)^4$, an injection spectrum $E^{-2.4}$ can fit the data, at least at energies above 10^{19} eV, requiring a luminosity per source above 10^{19} eV which is basically the same as in the non evolutionary case (but two orders of magnitude smaller if extrapolated down to 1 GeV). The small scale anisotropies are not appreciably affected by the evolution of the sources, because they are mainly determined by nearby sources ($z \leq 0.3$), and their number is fixed by the highest energy

events. In this case the density quoted above should be interpreted as the local density of sources.

The upcoming experiments such as the Pierre Auger Observatory and the EUSO Observatory will open many new avenues to determine the nature of the sources of UHECRs. We discussed here the potentials of these two experiments, with the help of numerical simulations for the propagation of UHECRs, that allowed us to simulate the expected statistics of events.

The two point correlation function is used to study the clustering properties of the events generated from sources having the density obtained from the analysis of the AGASA data. We find that the correlation function with the statistics of events expected with Auger shows a very pronounced peak at small scales, confirming the point-like nature of the sources.

For the case of Auger, the two point correlation function of events with energy above 4×10^{19} may not be the best tool to infer the point-like nature of the sources. In fact in the ~ 2 degrees of average angular resolution of the experiment doublets and triplets of events occur at random, not necessarily due to the point-like nature of the sources, but rather due to the abundance of events. In other words the multiplets often result from the contribution of different sources.

A better result is obtained by calculating the two point correlation function limited to the events with energy above 10^{20} eV. In this case the calculated error bars appear to be small enough to allow the source counting with an uncertainty of one order of magnitude or less. A corresponding uncertainty has to be expected in the estimate of the luminosity of single sources.

The analysis based upon the calculation of the two point correlation function was also carried out for the EUSO expected statistics of events above 10^{20} eV. Besides the peak at small angular scales, the two point correlation function shows now a series of peaks that are not due to fluctuations in the number of events as they would result from propagation. These peaks are due to Poisson noise around the average of the correlation function at large angles, due to fluctuations in the number of sources in a given area. The wiggles disappear if one averages the correlation function over a large number of realizations of the source distribution. Although the peaks are washed out by statistical averaging, the information about the sources does not disappear, but remains in the amplitude of the fluctuations around the mean of the correlation function. The peaks provide us with another valuable tool to estimate the number density of the sources, with an uncertainty of at most one order of magnitude.

The important insight behind the appearance of this structure in the two point correlation function is that a *critical exposure* exist, which depends upon the source density in the sky, such that experiments with exposures larger

than the critical one are able to receive at least one event from each source. This is the reason why the peaks introduced above do not appear in smaller experiments but start to show up in EUSO if the source density is at the level of 10^{-5} Mpc^{-3} .

This insight allows for a direct counting of the sources in the sky through the identification of the clusters of events associated with each source. Our simulations show that this procedure should allow one to count the sources and therefore determine their density with uncertainties within 20 – 30%.

The nearby sources appear as blob-like structures in the sky, and some of them have very high multiplicity, up to $\sim 50 - 70$ at energies above 10^{20} eV. It is therefore proposed that the spectrum of the sources can be measured for the first time, also allowing the evaluation of the source distance. If this goal can be achieved, it would represent the first clear identification of the source itself, independently of the detection of the same source at other wavelengths.

The value of the source density that has been found here is comparable with the typical density of cosmic objects such as rich clusters of galaxies and active galactic nuclei. While the former cannot accelerate particles to the highest energies, active galaxies of some type might do it. It is therefore worth pursuing the investigation of the acceleration mechanisms in these sources.

Acknowledgments

We thank Roberto Aloisio, Venya Berezhinsky, Stefano Gabici, Angela Olinto and Mario Vietri for many useful discussions and ongoing collaboration. We are also grateful to William Burgett for a useful correspondence, to Alessandro Petrolini for valuable comments to the manuscript and to Andrea Ferrara and Evan Scannapieco for a very useful discussion on correlation functions. We are also grateful to the anonymous referee for constructive comments. This work was partially supported through grant COFIN-2002 at Arcetri.

References

- [1] P.G. Tinyakov and I.I. Tkachev, JETP Lett. **74** (2001) 445; Pisma Zh. Eksp. Teor. Fiz. **74** (2001) 499
- [2] D. Gorbunov, P. Tinyakov, I. Tkachev and S. Troitsky, Astrophys. J. Lett. **577** (2002) L93
- [3] D. De Marco, P. Blasi and A.V. Olinto, Astropart. Phys., in press (preprint astro-ph/0301497)

- [4] T. Abu-Zayyad, et al., preprint astro-ph/0208301
- [5] T. Abu-Zayyad, et al., preprint astro-ph/0208243
- [6] Y. Uchihori, M. Nagano, M. Takeda, M. Teshima, J. Lloyd-Evans and A.A. Watson, *Astropart. Phys.* **13** (2000) 151
- [7] D. Harary, S. Mollerach and E. Roulet, *JHEP* **2** (2000) 035
- [8] H. Goldgerg and T.J. Weiler, *Phys. rev.* **D64** (2001) 056008
- [9] W.S. Burgett and M.R. O'Malley, *Phys. Rev.* **D67** (2003) 092002
- [10] S.L. Dubovsky, P.G. Tinyakov and I.I. Tkachev, *Phys. Rev. Lett.* **85** (2000) 1154
- [11] Z. Fodor and S.D. Katz, *Phys.Rev.* **D63** (2001) 023002
- [12] J. W. Cronin, *Proceedings of ICRC 2001* (2001).
- [13] see <http://www.euso-mission.org>
- [14] H. Yoshiguchi, S. Nagataki, S. Tsubaki and K. Sato, *Astrophys. J.* **586** (2003) 1211
- [15] H. Yoshiguchi, S. Nagataki and K. Sato, preprint astro-ph/0302508
- [16] T. Stanev, preprint astro-ph/0108338
- [17] C. Isola and G. Sigl, *Phys. Rev.* **D66** (2002) 3002
- [18] G. Sigl, F. Miniati and T. Ensslin, preprint astro-ph/0302388
- [19] M. Blanton, P. Blasi and A. V. Olinto, *Astropart. Phys.* **15** (2001) 275
- [20] G. R. Blumenthal, *Phys. Rev.* **D1** (1970) 1596.
- [21] M. J. Chodorowski, A. A. Zdziarski, and M. Sikora, *Astrophys. J.* **400** (1992) 181.
- [22] P. Bhattacharjee and G. Sigl, *Phys. Rept.* 327 (2000) 109
- [23] T. Stanev, R. Engel, A. Mucke, R. J. Protheroe and J. P. Rachen, *Phys. Rev. D* **62** (2000) 093005.
- [24] V. Berezhinsky and S. Grigorieva, *Astron. Astroph.* 199 (1988) 1
- [25] V. S. Berezhinsky, S.V. Bulanov, V. A. Dogiel, V. L. Ginzburg, and V. S. Ptuskin, *Astrophysics of Cosmic Rays*, (Amsterdam: North Holland, 1990)
- [26] V. Berezhinsky, A. Z. Gazizov and S. Grigorieva, preprint astro-ph/0210095
- [27] V. Berezhinsky, A. Z. Gazizov and S. Grigorieva, preprint hep-ph/0204357
- [28] M. Takeda, et al., *Astrophys. J.* **522** (1999) 225
- [29] N. Hayashida et al., *Astrophys. J.* **522** (1999) 225

- [30] P. Sommers, *Astropart. Phys.* **14** (2001) 271
- [31] P. Blasi, S. Burles and A.V. Olinto, *Astrophys. J. Lett.* **514** (1999) 79
- [32] K.-T. Kim, P.P. Kronberg, G. Giovannini and T. Venturi, *Nature* **341** (1989) 720
- [33] V. Berezhinsky, A. Z. Gazizov and S. Grigorieva, preprint astro-ph/0302483
- [34] T.E. Clarke, P.P. Kronberg and H. Böhringer, *Astrophys. J. Lett.* 547 (2001) 111